Dust

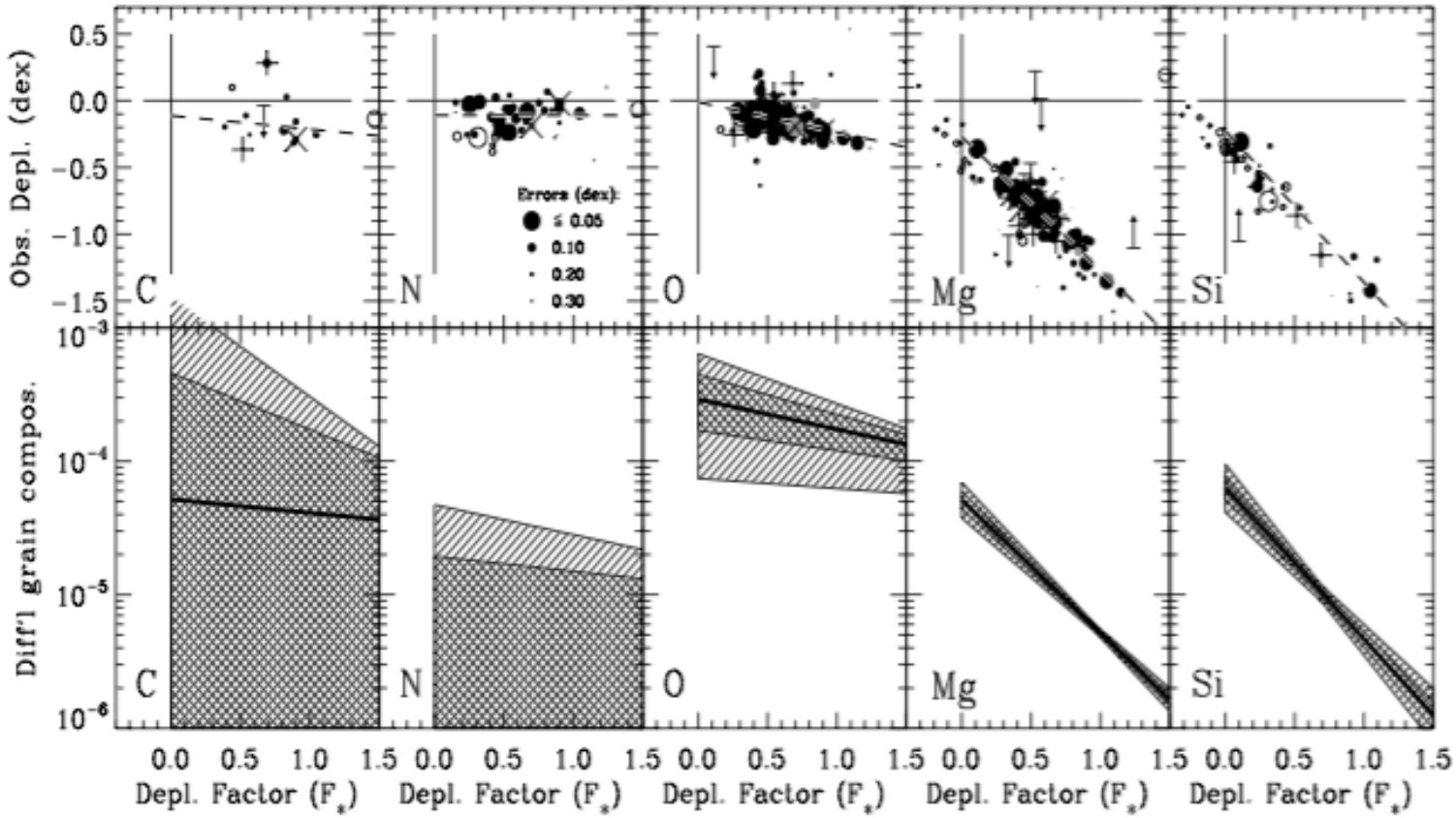

Figure 5. Top row of panels: measured depletions (points) and the linear trends defined by the parameters A_X, B_X, and z_X in Equation (10) (dashed lines), as listed in Table 4, shown as a function of the generalized depletion parameter F_* for the elements C, N, O, Mg, and Si. The solid points have $N(\mathrm{H}) > 10^{19.5}\,\mathrm{cm}^{-2}$, while open ones have N(H) values below this range. The gray points represent sightlines that had only three elements to define their F_* parameters, while the black ones represent those that had four or more elements. Upper and lower limit measurements are depicted with the arrows (and were not included in any analysis). Sight lines that crossed the galactocentric limits $R_{GC} < 7$ kpc or $R_{GC} > 10$ kpc are overlaid with crosses (+) or x's (×), respectively, to indicate that they were not used to define the linear trends for the elements. Bottom row of panels: differential consumptions of elements by number (relative to hydrogen) by dust grains for small changes in F_*, again plotted as a function of F_*. The trend lines that follow Equation (21) with the best values of A_X and B_X are shown with dark lines, while the allowable changes that can arise from the uncertainties in A_X and B_X are shown by the shaded regions. Uncertainties at the 1σ level are shown by the cross-hatched areas, while the envelopes for 2σ deviations have simple line shading in only one direction.

Jenkins 2009

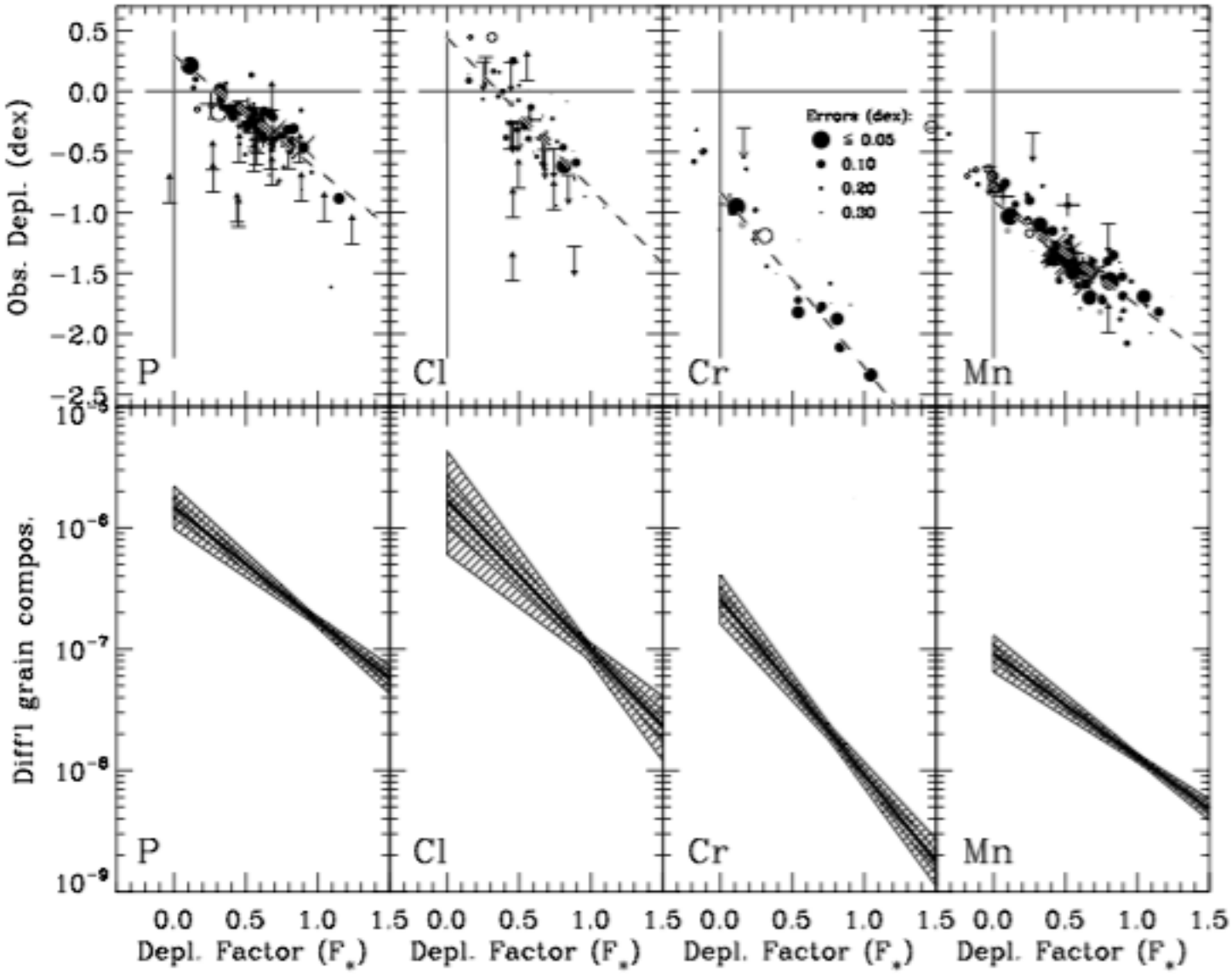
Obs. Depl. (dex)
0.5
0.0
−0.5
−1.0
−1.5
−2.0
−2.5
P
Cl
Cr
Mn
Errors (dex):
≤ 0.05
0.10
0.20
0.30
Diff'l grain compos.
10^{-5}
10^{-6}
10^{-7}
10^{-8}
10^{-9}
P
Cl
Cr
Mn
0.0 0.5 1.0 1.5
Depl. Factor (F_*)
Depl. Factor (F_*)
Depl. Factor (F_*)
Depl. Factor (F_*)

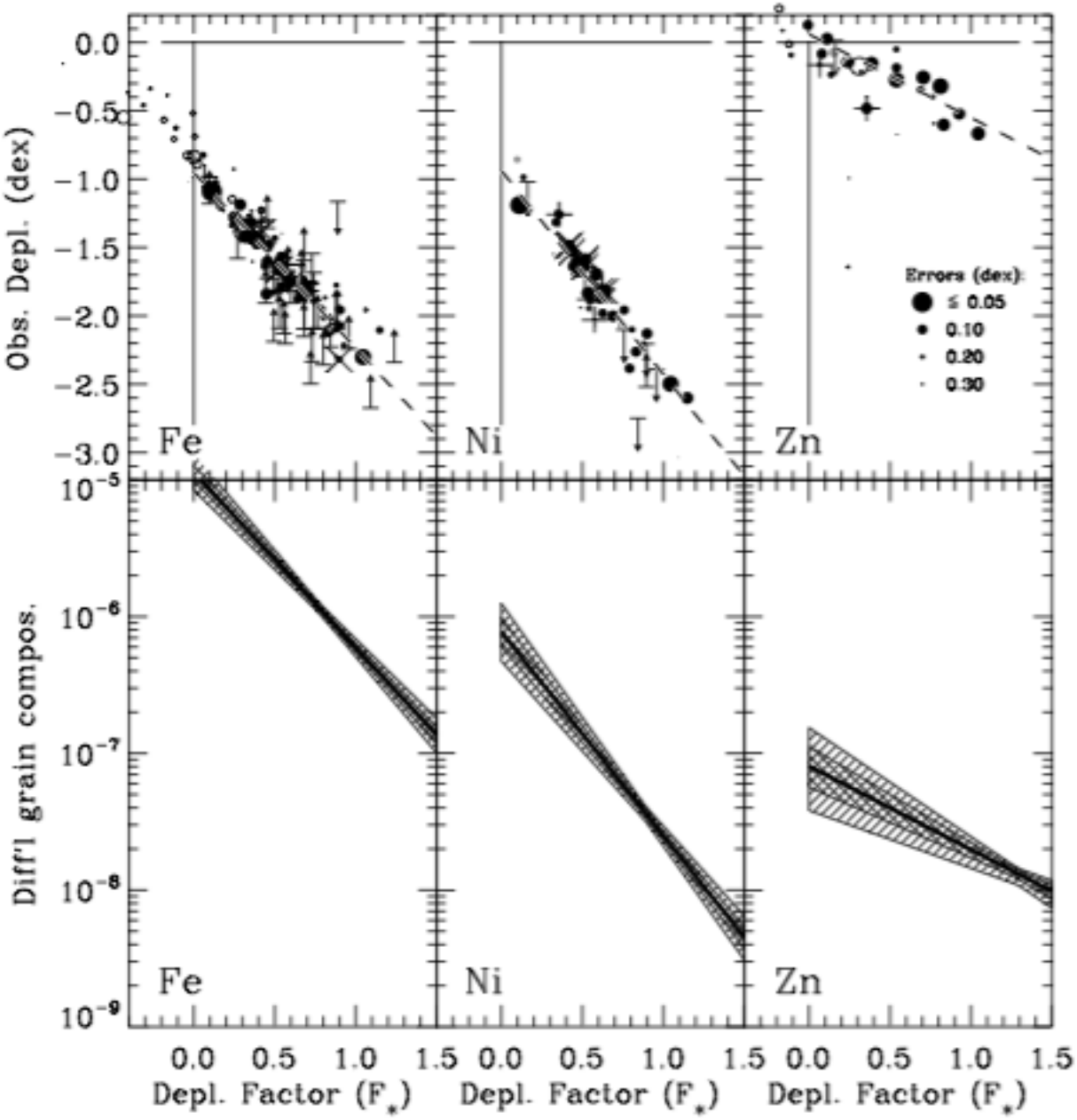
Obs. Depl. (dex)
0.0
−0.5
−1.0
−1.5
−2.0
−2.5
−3.0
Fe
Ni
Zn
Errors (dex):
≤ 0.05
0.10
0.20
0.30
Diff'l grain compos.
10^{-5}
10^{-6}
10^{-7}
10^{-8}
10^{-9}
Fe
Ni
Zn
0.0 0.5 1.0 1.5
Depl. Factor (F_*)
0.0 0.5 1.0 1.5
Depl. Factor (F_*)
0.0 0.5 1.0 1.5
Depl. Factor (F_*)

Calculated extinction for the present grain model (*heavy solid line*) and the observed average ($R_V \approx 3.1$) interstellar extinction curve (*dotted line*—Fitzpatrick 1999; *open circles*—Mathis 1990). Model results are the sum of four components: "B_{sil}" (silicate, $a \geq 250$ Å; *long-dashed line*); "S_{sil}" (silicate, $3.5 \leq a \leq 250$ Å; *short-dashed line*); "B_{carb}" (carbonaceous, $a \geq 250$ Å; *dot-dashed line*); and "S_{carb}" (carbonaceous, $3.5 \leq a \leq 250$ Å, including PAHs; *thin solid line*). The upper right inset illustrates the aromatic 6.2 μm absorption feature and the 9.7 μm silicate band. The narrow feature at 11.5 μm is caused by a lattice mode of crystalline graphite (Draine 1984) and would likely be smoothed out in an imperfect polycrystalline sample. The lower left inset plots the extinction curve against λ^{-1} (μm^{-1}).

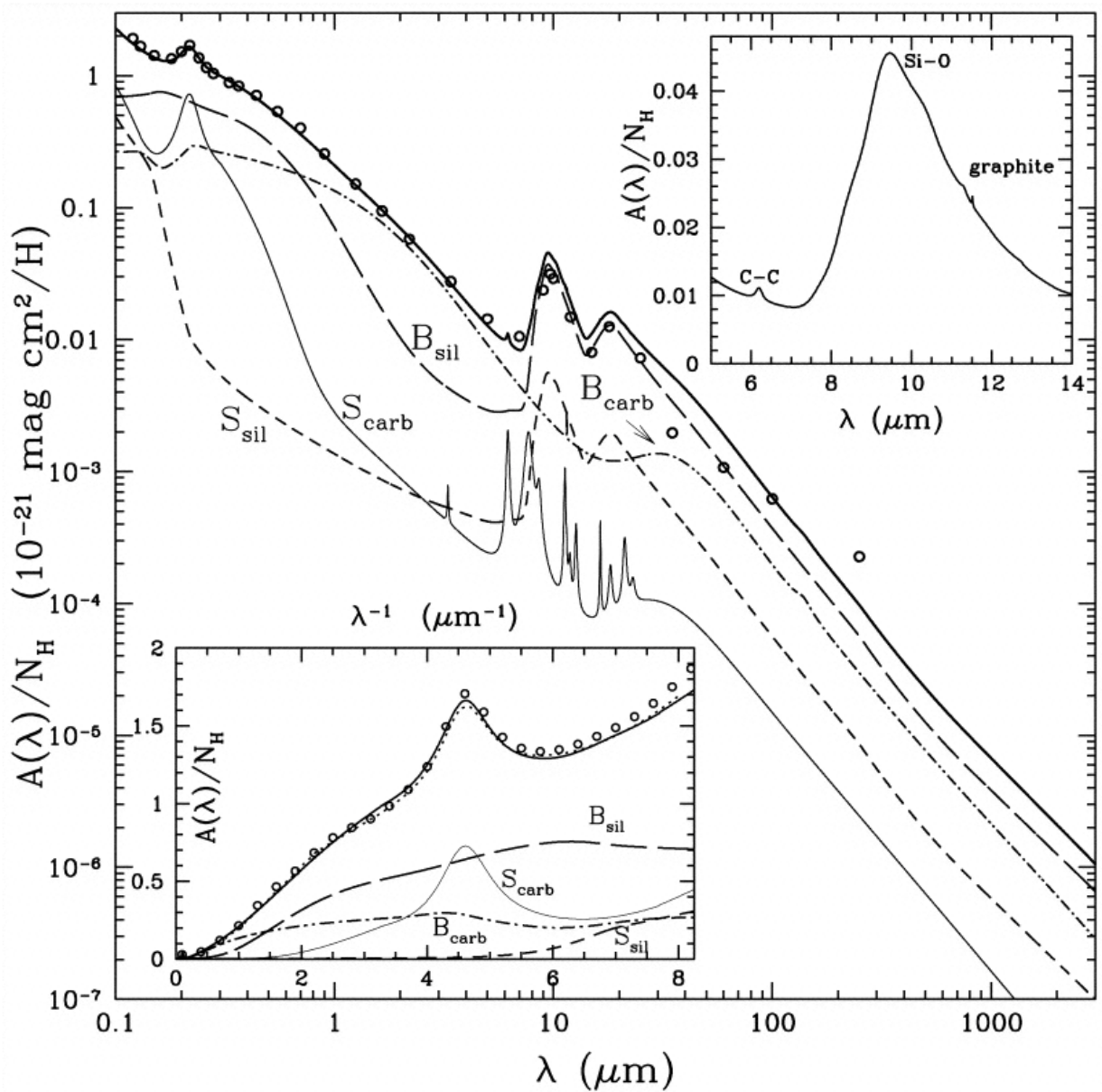

Draine & Li (2002)

Comparison of the model to the observed emission from the diffuse ISM at high Galactic latitudes ($|b| \geq 25°$). Curves labeled B_{sil} and B_{carb} show emission from "big" ($a \geq 250$ Å) silicate and carbonaceous grains; curves labeled S_{sil} and S_{carb} show emission from "small" ($a < 250$ Å) silicate and carbonaceous grains (including PAHs). Triangles show the model spectrum (*solid curve*) convolved with the DIRBE filters. Observational data are from DIRBE (*diamonds*; Arendt et al. 1998) and FIRAS (*squares*; Finkbeiner et al. 1999).

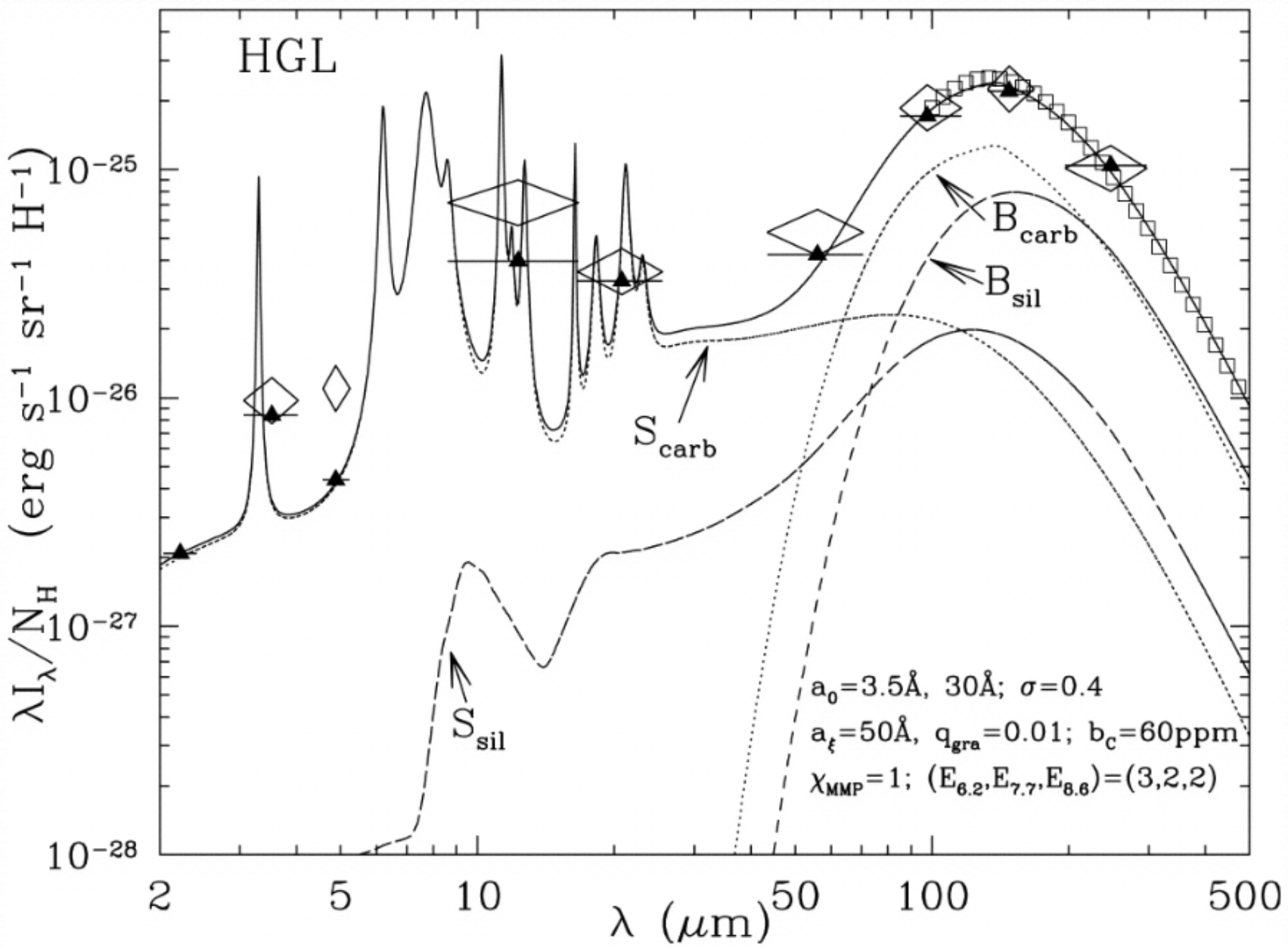

Case A grain-size distributions for $R_V = 3.1$. The values of b_C are indicated. The heavy, solid lines are the MRN distribution, for comparison. Our favored distribution has $b_C = 6 \times 10^{-5}$ (see text).

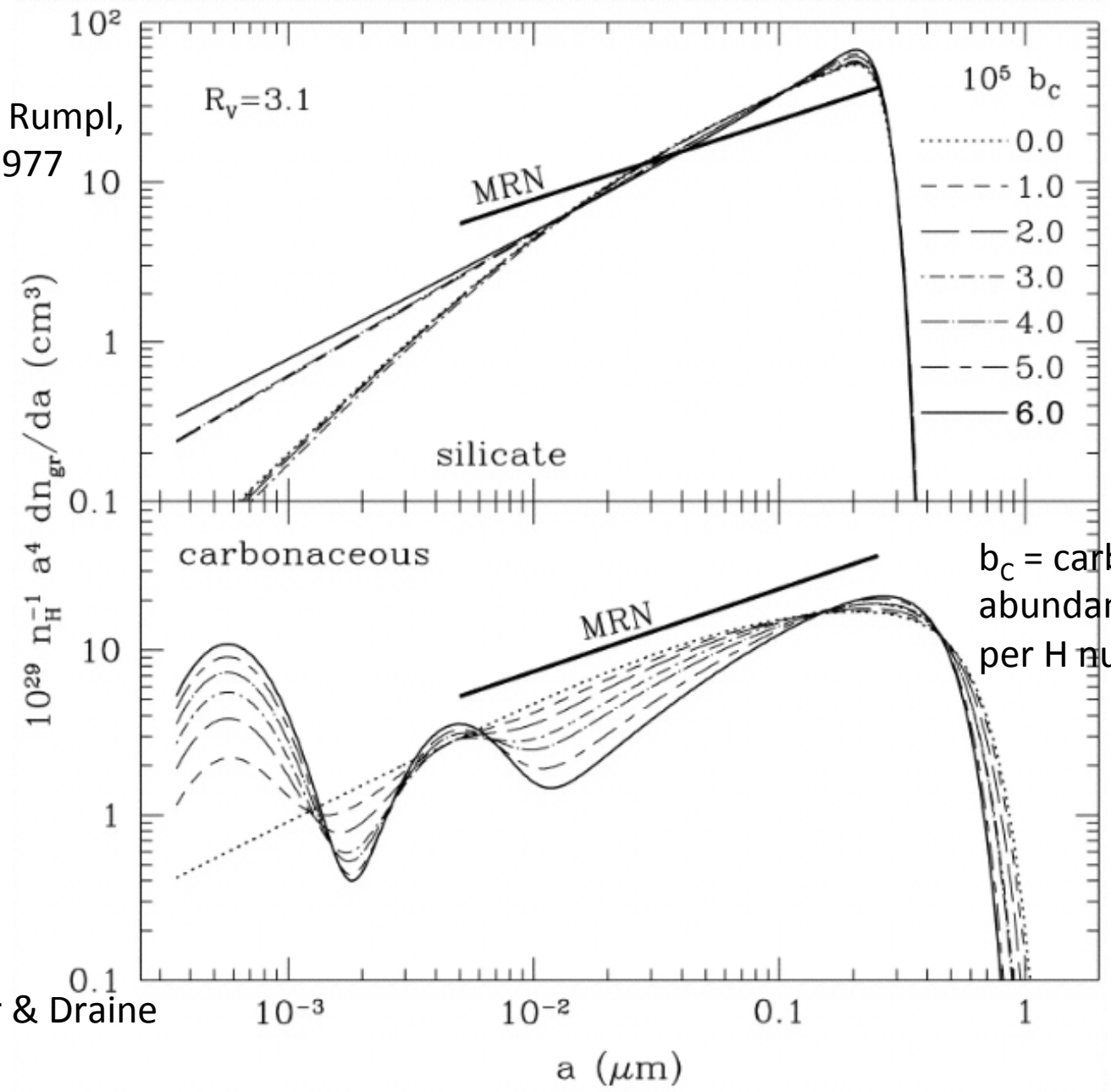

MRN=Mathis, Rumpl, & Nordsieck 1977

b_C = carbon abundance in dust per H nucleus

Weintgarner & Draine 2001

Equilibrium temperatures for graphite (*dotted lines*) and silicate grains (*solid lines*) in environments with various starlight intensities.

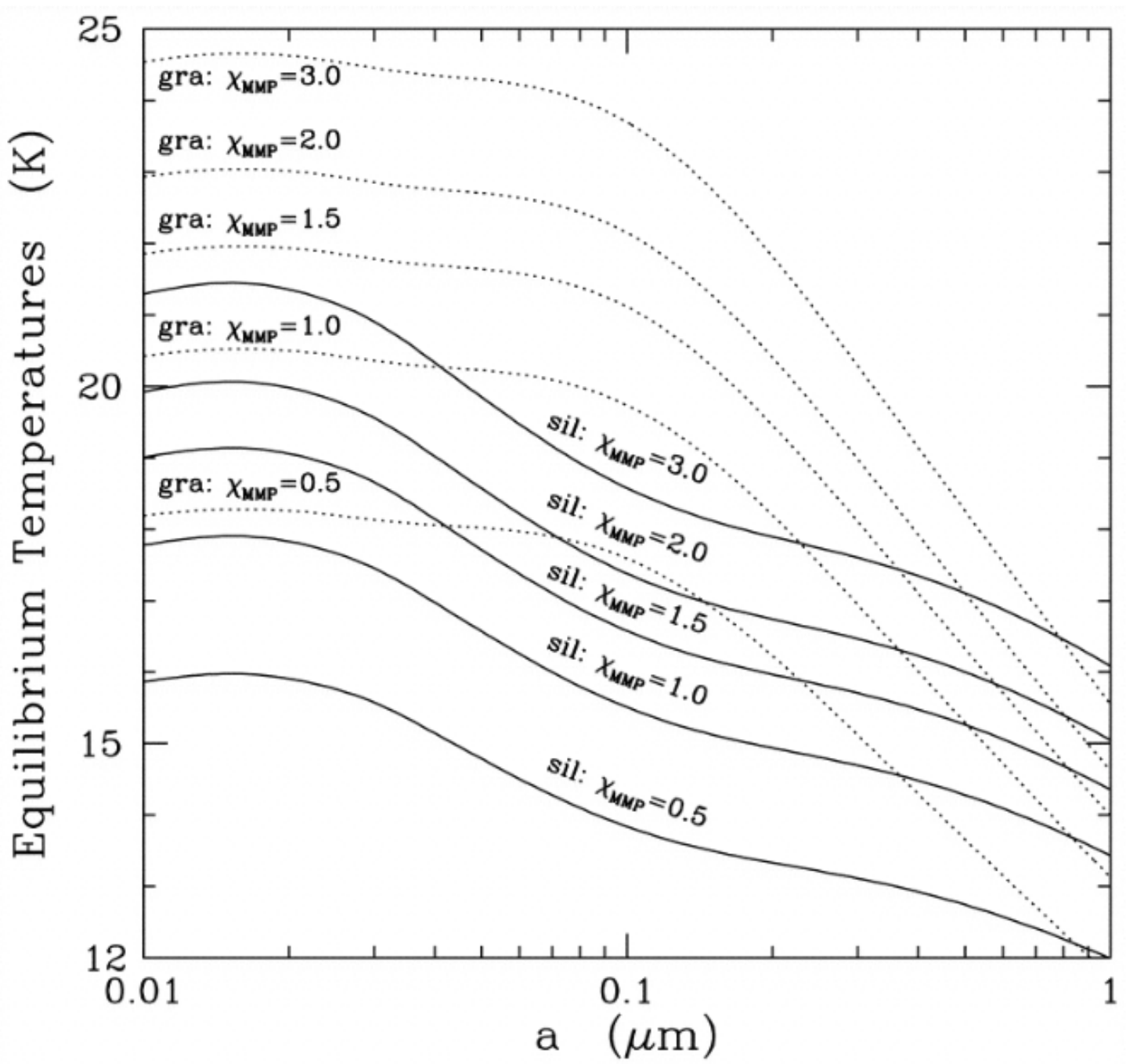

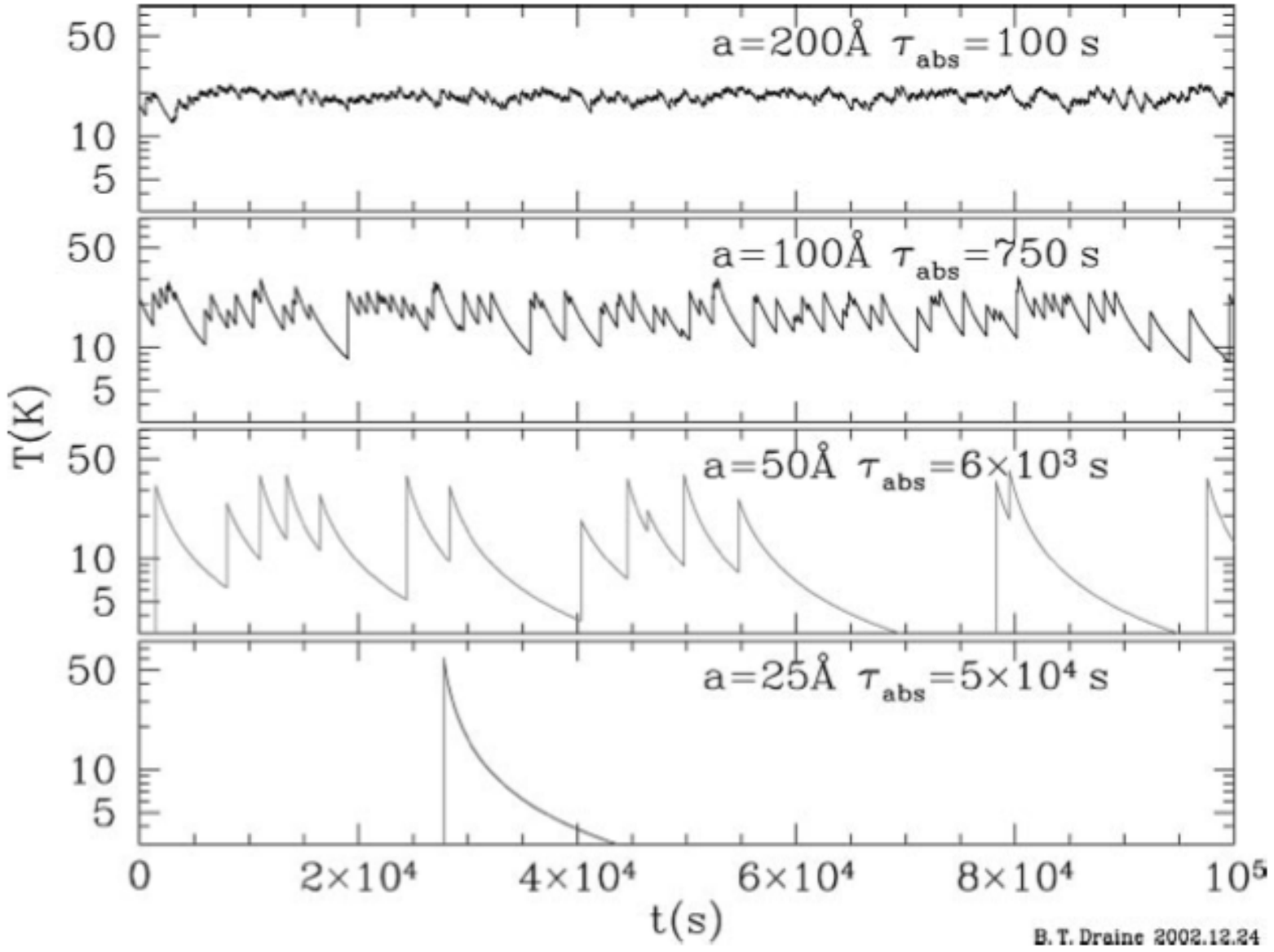

Figure 13 A day in the life of four carbonaceous grains, heated by the local interstellar radiation field. τ_{abs} is the mean time between photon absorptions (Draine & Li 2001).

IR emission spectra for small carbonaceous grains of various sizes heated by starlight with $\chi_{MMP} = 1$, calculated using the full energy distribution function $P(E)$ (*solid lines*); also shown (*broken lines*) are spectra computed for grains at the "equilibrium" temperature $\bar{T}$. Transient heating effects lead to significantly more short wavelength emission for $a \lesssim 200$ Å.

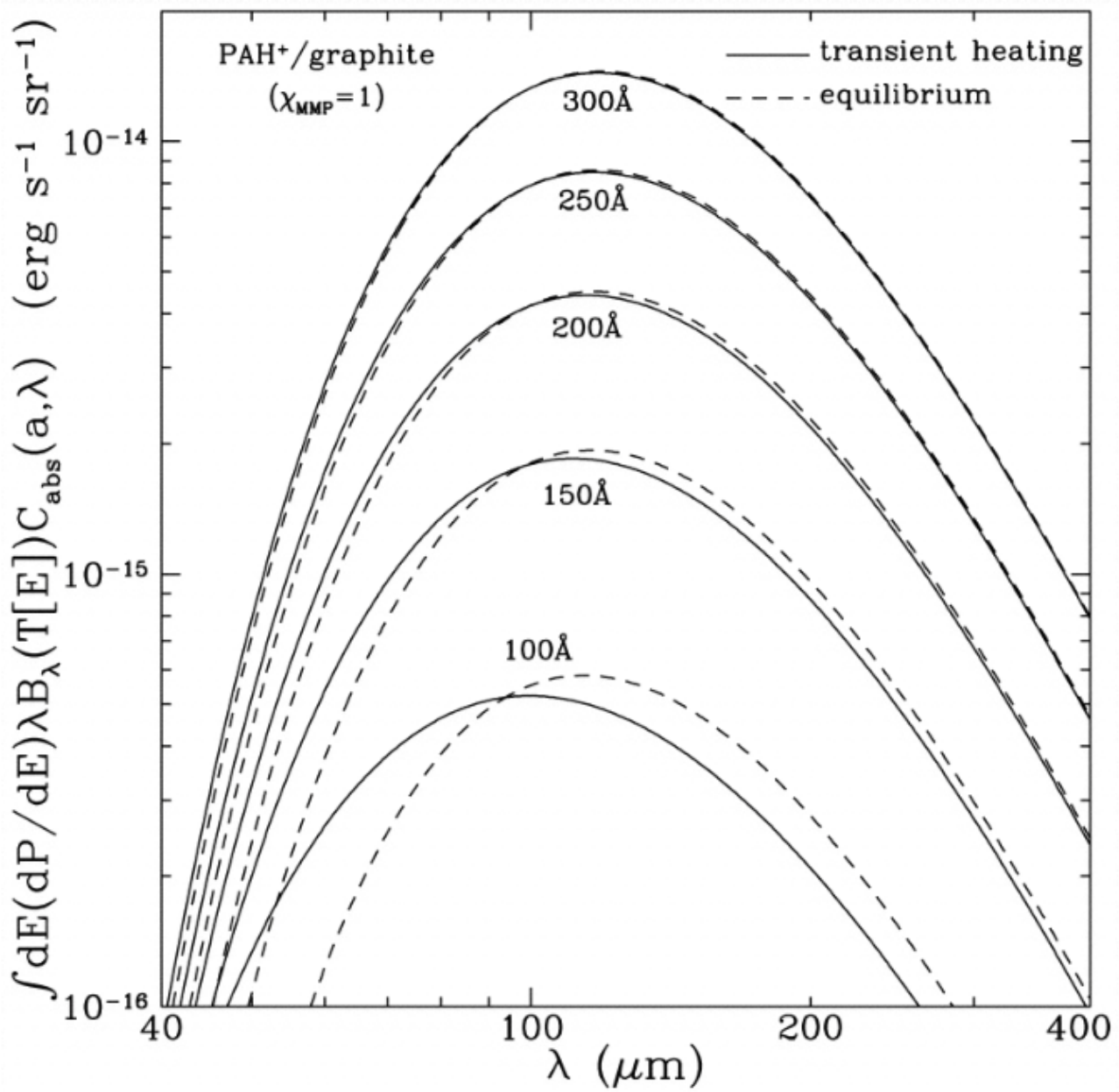

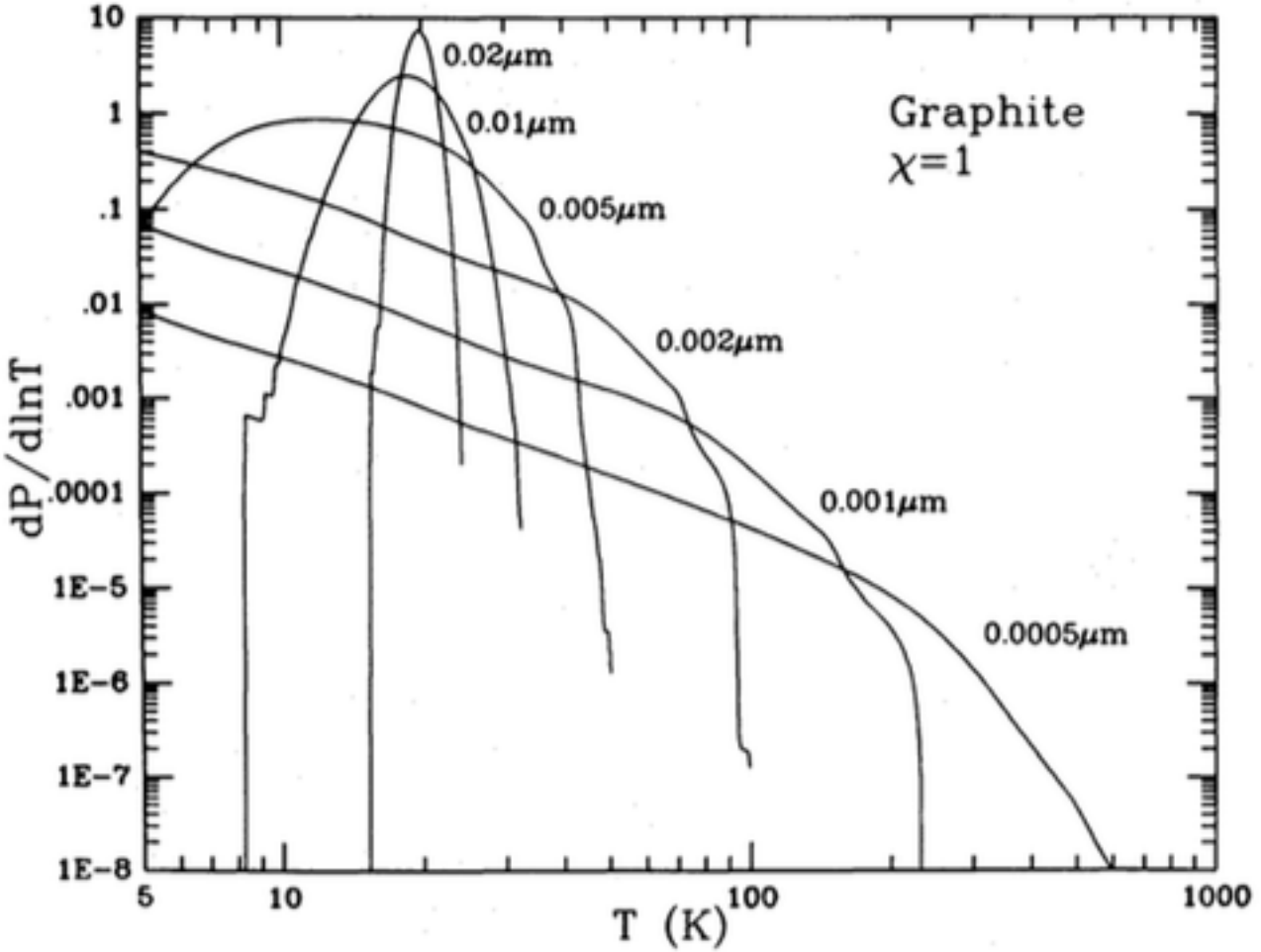

FIG. 1.—Temperature distribution functions $dP/d \ln T$ for graphite grains of various radii a, exposed to the average interstellar radiation field ($\chi = 1$). Here $P(T)$ is the probability of finding the grain at a temperature greater than T. Curves are labeled by a.

Draine & Anderson 1985